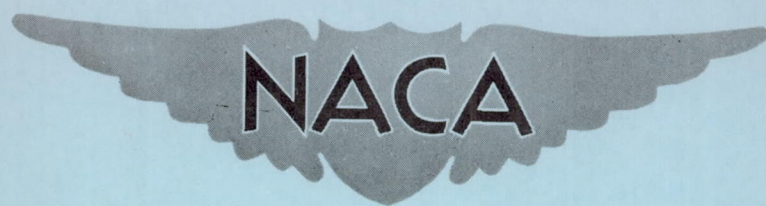


CONFIDENTIAL

Copy 259
RM E55J18

NACA RM E55J18



RESEARCH MEMORANDUM

EXPERIMENTAL EVALUATION OF GASEOUS HYDROGEN FUEL
IN A 16-INCH-DIAMETER RAM-JET ENGINE

By E. E. Dangle and William R. Kerslake

Lewis Flight Propulsion Laboratory
Cleveland, Ohio

CLASSIFICATION CHANGED TO UNCLASSIFIED
AUTHORITY: NASA TECHNICAL ANNOUNCEMENTS NO. 45
EFFECTIVE DATE: 10/1/65

CLASSIFIED DOCUMENT - TITLE UNCLASSIFIED

This material contains information affecting the national defense of the United States within the meaning of the espionage laws, Title 18, U.S.C., Secs. 793 and 794, the transmission or revelation of which in any manner to an unauthorized person is prohibited by law.

**NATIONAL ADVISORY COMMITTEE
FOR AERONAUTICS**

WASHINGTON

March 6, 1956

Reclassified May 29, 1959

CONFIDENTIAL

NATIONAL ADVISORY COMMITTEE FOR AERONAUTICS

RESEARCH MEMORANDUMEXPERIMENTAL EVALUATION OF GASEOUS HYDROGEN FUEL
IN A 16-INCH-DIAMETER RAM-JET ENGINE *

By E. E. Dangle and William R. Kerslake

SUMMARY

The combustion efficiency of gaseous hydrogen fuel was determined in a 16-inch-diameter ram-jet engine in a connected-pipe test facility. Operating conditions simulated Mach numbers of 2.5 and 3.0 at altitudes of 51,000 to 66,000 feet and 63,000 to 89,000 feet, respectively. Combustor modifications included two fuel-injector designs, several combustor lengths, and tests with and without flameholders. Combustion efficiencies were measured by three techniques: a heat balance after adding quench water, direct temperature measurement by thermocouples, and total-pressure measurements at the exit of a choked convergent exhaust nozzle. The agreement among the three methods was reasonably good.

A combustor length of only 16 inches gave combustion efficiencies of 90 percent or greater for equivalence ratios from 0.5 to stoichiometric. The engine started at pressures as low as 7 inches of mercury absolute and ran very smoothly at all operating conditions.

INTRODUCTION

The analytical investigations of references 1 and 2 have shown that the high heating value of hydrogen and its stable burning quality over wide ranges of pressure and fuel-air ratio make hydrogen a desirable fuel for long-range high-altitude ram-jet application. Furthermore, the refrigerant capacity of liquid hydrogen makes it particularly attractive as a coolant for high-speed flight application.

The high flame speeds associated with hydrogen indicate the probability of high combustion efficiencies along with high heat-release rates. This, in turn, would indicate that the combustor designed to burn hydrogen could be considerably shorter than a hydrocarbon combustor and still operate with high, if not higher, combustion efficiency. Because so little information is available on the combustion characteristics of hydrogen under conditions similar to those encountered in an

*Title, Unclassified.

actual ram-jet combustor, an investigation was made to evaluate the combustion efficiency of gaseous hydrogen in a ram-jet combustor and to establish a combustor design for further study in a supersonic tunnel facility.

The following conditions were investigated with a 16-inch-diameter ram-jet engine in a connected-pipe facility: combustor inlet pressure of 13 to 50 inches mercury absolute; inlet velocity of 110 to 340 feet per second based on a 16-inch-diameter cross section; inlet air temperatures of 120° , 230° , and 640° F. The two lower temperatures correspond to conditions in a particular supersonic wind tunnel at Mach numbers of 2.5 and 3.0, respectively. The highest temperature simulates a flight Mach number of 3.0 above the tropopause.

3912

APPARATUS

Engine installation. - The installation of the 16-inch-diameter ram-jet engine in the pipe facility is shown in figure 1. The combustor length, varied during the test program, was measured from the fuel-injector tubes to either a quench water spray or the throat of a convergent exhaust nozzle. The engine was mounted in a connected-pipe setup and exhausted through an ejector system. Air flow to the engine was controlled by a butterfly valve upstream of the engine and was metered by an orifice in the supply line. The inlet air was heated to 120° or 230° F by a gas-fired heat exchanger, and to 640° F by a combustor placed directly in the air line. The air contained combustion products 0 to 8 percent by weight as a result of putting the combustor (assumed 100-percent efficient) in the air line; oxygen concentration varied from 23 to 21 percent by weight. The ram-jet-engine exhaust gases were cooled in a calorimeter consisting of a water-spray quench section and water-cooled outlet duct. The resulting gas and steam temperatures were measured.

Fuel-injection system. - The hydrogen fuel was supplied in cylinders with total capacities of 420 pounds of hydrogen and gas pressure of 2400 pounds per square inch gage. The fuel was taken directly from the cylinders through pressure reducing valves, a metering orifice, and a throttling valve to the engine. Gas analysis of the hydrogen indicated it was more than 99 percent pure.

Two fuel-injector designs were used in the investigation. The first fuel injector consisted of three concentric rings with six supply struts. The rings were split into six equal sectors, and a total of 432 injection holes, 0.055 inch in diameter, were drilled as shown in the sector in figure 2(a). Nine-tenths of the fuel sprayed cross stream, while the remainder sprayed downstream.

The second fuel injector consisted of 12 radial spray bars equally spaced around the combustor. Figure 2(b) shows one of these spray bars. Each bar contained 14, 3/32-inch-diameter fuel orifices spraying cross stream and located at centers of equal duct areas. Hydrogen flow was choked at the injection holes of both injectors over the entire fuel flow range.

Engine configurations. - Changes in the centerbody design, fuel injectors, flameholders, burner length, and exhaust nozzle area resulted in the following engine configurations:

Combustor components	Engine configurations		
	A	B	C
Centerbody design	Tapered to a point-taper at 25° angle (fig. 3(a))	Tapered to a 2-inch-diameter stub-taper at 25° angle (fig. 3(b))	A 1/6-sector of configuration A (5/6 of configuration A blocked-off). Engine centerbody served as bottom wall to 1/6-sector (fig. 3(c))
Fuel injectors	3 concentric-ring injectors (fig. 2(a)) blocking 17 percent of engine open area	12 radial injectors (fig. 2(b)) blocking 10 percent of engine open area	3 concentric-ring injectors (fig. 2(a)) blocking 17 percent of sector open area
Flameholder	No flameholder	6 radial V-gutters (fig. 2(c)), blocking 20 percent of engine open area, used only in run 10; remaining runs without flameholders	No flameholder
Exhaust-nozzle area and combustor length (combustor length defined as distance from fuel injectors to water sprays, unless otherwise specified)	(a) 0.5 nozzle (11.3-inch-diameter); combustor length, 26 inches (fuel injectors to thermocouples) (b) 1.0 nozzle (16-inch-diameter); combustor length, 28 inches (c) 1.0 nozzle (16-inch-diameter); combustor length, 16 inches	(a) 0.5 nozzle (11.3-inch-diameter); combustor length, 36 inches (fuel injectors to thermocouples) (b) 1.0 nozzle (16-inch-diameter); combustor length, 44 inches	No exit restrictions; combustor length, 26 inches (fuel injectors to thermocouples)

Instrumentation. - A water-cooled total-pressure rake was located so that the pressure tubes were in the plane of the engine exhaust nozzle throat. The rake consisted of 15 total-pressure tubes located in the centers of 7 equal areas. Pressures from the rake were measured with a strain-gage pressure transducer and recorded on a moving strip chart. Static pressure was measured at the throat of the nozzle and 1 inch downstream of the nozzle at the 16-inch-diameter wall. The combustor inlet static pressure was measured where the centerbody was 8 inches in diameter for configuration A, and 7 inches in diameter for configuration B.

3912

Bare-wire chromel-alumel thermocouples were located 1/4-inch downstream of the plane of the engine exhaust nozzle throat. Direct temperature measurements were made with 16, 34, and 44 thermocouples. For those runs in which 16 thermocouples were used, only one quadrant of the exhaust nozzle was instrumented; when 34 and 44 thermocouples were utilized, the entire nozzle was uniformly instrumented. The heat-balance thermocouple station was located 24 feet downstream of the engine exhaust nozzle. This thermocouple station consisted of 16 thermocouples located in the centers of equal areas across the 24-inch-diameter exhaust duct.

PROCEDURE

Operating conditions. - The following table indicates the range of combustor inlet conditions over which the engine was operated and the corresponding simulated flight conditions.

Inlet-air static pressure, in. Hg abs	23 to 45	20 to 45	13 to 45
Inlet-air temperature, °F	120*	230*	640
Inlet Mach number	0.171 to 0.094	0.220 to 0.070	0.214 to 0.115
Simulated flight Mach number	2.5	3.0	3.0
Simulated flight altitude, ft	66,000 to 51,000	80,000 to 63,000	89,000 to 63,000

* Maximum temperature for supersonic wind tunnel at corresponding Mach number.

Air mass flow was set at 15.2 pounds per second corresponding to critical air flow in the 16-inch engine at a wind tunnel condition of Mach number

3.0 and altitude 72,000 feet. Because of the limited capacity of the exhaust system, the engine air mass flow was reduced to 7.6 pounds per second for the low-pressure tests. The exhausting ejectors were run at full capacity to obtain the minimum combustor pressure for each data point.

Combustion efficiencies. - Three techniques for obtaining combustion efficiency were concurrently used in most of the runs. The engine was started at lean equivalence ratios, and the equivalence ratio was then increased in steps to the maximum equivalence ratio. Equivalence ratio is the metered fuel-air ratio divided by the stoichiometric fuel-air ratio of 0.0294 for hydrogen and air. The engine was operated at each equivalence ratio while data for all three methods of instrumentation were taken. The three methods employed were heat balance (calorimeter), direct temperature, and total pressure.

The heat-balance system is similar to the method outlined in reference 3. Combustion efficiency is defined as the ratio of the enthalpy change of fuel, air, quench water, and engine cooling water to the theoretical lower heating value of the gaseous fuel (51,571 Btu/lb). This method was employed throughout the entire equivalence-ratio range.

Direct temperature measurements of the exhaust gases were made up to equivalence ratios of approximately 0.35, at which point the thermocouples began burning out. From the averaged, corrected, total temperatures at the nozzle throat (see appendix), the enthalpy of the exhaust products was determined from a plot of combustion temperature against equivalence ratio. Combustion efficiency was then defined as the ratio of the enthalpy of the exhaust products to the theoretical lower heating value of the gaseous fuel.

Total pressures, measured at the throat of a choked nozzle, were used to calculate a total temperature (see appendix), and the combustion efficiency was determined as with the total-temperature method. The total-pressure method was employed only with the 0.5 area exhaust nozzle and then only when this nozzle was choked. The nozzle was assumed choked when the exhaust-nozzle pressure ratio was 2.15 and greater. This lower limit for the nozzle pressure ratio is taken from reference 4.

RESULTS AND DISCUSSION

The performances of the three configurations for all operating conditions are summarized in table I. In general, the combustion efficiencies of the three configurations were 90 percent or greater in the higher equivalence-ratio regions (0.4 to 1.0); in the lean regions (0.4 and lower) the efficiencies fell off and in some cases rather rapidly. The combustion efficiencies determined from the three methods of instrumentation (heat balance, thermocouple, and total pressure) are also presented in table I and are generally in good agreement.

Effect of Inlet Parameters and Design Variables

on Combustion Efficiencies

Effect of temperature. - For equivalence ratios of 0.5 and greater, a change in inlet-air temperature from 230° to 640° F had no effect on the combustion efficiencies of configuration A (fig. 4(a)). A 95-percent combustion-efficiency level was maintained from equivalence ratios of 0.5 to 0.9. However, at the lean equivalence ratios, the curve for 230° F fell off more rapidly than the one for 640° F.

The effect of inlet-air temperature on configuration A was somewhat obscured by a change in the distance of fuel spray to water quench which coincided with the change in air temperature. Data taken with 230° F inlet air were obtained with a 34-inch combustor length, whereas those for 640° F were with a 28-inch combustor length. The distance between the fuel injectors and the thermocouples remained constant. The combustion efficiencies determined from the direct thermocouple measurements were in agreement with the heat-balance efficiencies, which indicates that the combustor length had no effect on the heat-balance efficiencies because combustion was essentially complete at the thermocouple station.

Figure 4(b) is a comparison of the combustion efficiencies of configuration B with 120°, 230°, and 640° F inlet-air temperatures. No effect of inlet-air temperature is apparent. The peak efficiency of the curve faired through the data points was 94 percent at equivalence ratios of 0.5 to 0.7. There was a small drop at rich operation, however, and the fall-off in efficiency for lean operation was shifted to an equivalence ratio of 0.3. Configuration B had a combustor length of 44 inches.

Effect of pressure. - The effect of combustor inlet-air pressure on the combustion efficiency of configuration A is shown in figure 5(a). For equivalence ratios above 0.7, the efficiency for inlet pressures from 13.2 to 22.6 inches of mercury absolute (run 7) is about 3 percent less than the efficiency for pressures from 28.8 to 50.5 inches of mercury absolute (run 2). Below 0.7 equivalence ratio, efficiency at the lower pressures drops off rapidly but has a peculiar rise below 0.3 equivalence ratio. This unusual rise in combustion efficiency could be due to instrument error but is corroborated by both the heat-balance efficiencies and the direct-temperature efficiencies. Similar rises in the lean range were also noted in the data of runs 3, 4, and 6. The combustor length for the pressure investigation was 28 inches, and burner inlet velocities ranged between 340 to 184 feet per second for both high-pressure and low-pressure operation. It was possible to maintain similar combustor-inlet velocities at the two pressure levels by varying the air flow to the engine.

Figure 5(b) compares configuration B at two combustor pressure levels, 25 to 45.7 inches of mercury absolute for high-pressure operation

and 19.9 to 34.6 inches of mercury absolute for low-pressure operation. There was no effect of pressure on the combustion efficiency in the range investigated. Runs 4 and 8 had the same air flow, but run 8 had a lower pressure range because the 1.0 engine exhaust nozzle was used.

Owing to the limited exhaust capacity of the test facility, a further decrease in combustor pressure could be achieved only by reducing combustor cross-sectional area and air flow. Accordingly, a 1/6-sector of configuration A, designated configuration C, was tested. The combustion efficiency of configuration C (fig. 5(c)) is based on direct-thermocouple measurement only. No heat-balance data are presented because equilibrium temperatures could not be established in the calorimeter section with the reduced mass flows and velocities. The data indicate that the combustion efficiency of the 1/6-sector at pressures of 9.2 to 11.4 inches of mercury absolute was 18 to 6 percent lower than configuration A at pressures of 23 to 45 inches of mercury absolute. However, the sector data are uncorrected for heat loss to the burner walls which, when accounted for, would probably increase the combustion efficiency another 6 percent. In view of these results, it appears that decreased pressures resulted in little decrease in combustion efficiencies up to an equivalence ratio of 0.3.

Effect of flameholder. - Figure 6 is a plot of the combustion efficiency of configuration B with a radial V-gutter flameholder (run 10) and without a flameholder (run 4). There was little improvement in the combustion efficiency when using the flameholder and the efficiency was even slightly decreased in the lean region. In the rich region, the combustion efficiencies for the combustor with a flameholder were slightly higher than the combustor efficiencies for the combustor without a flameholder. The flameholder was probably not a flameholding device at all, but rather a weak turbulence generator. The hydrogen possibly did not penetrate far enough to be caught in the recirculation zone of the V-gutter. A section of one of the concentric tubes of configuration A was run in a small test rig at similar conditions to the 16-inch engine. Sodium bicarbonate dust was introduced upstream of the fuel spray tube and the now-luminous flame was observed through a window. Flame seated at each of the injection holes in the fuel spray tube, but penetrated less than 1/8 inch into the air stream after flowing 1 inch downstream.

A flameholder in the usual sense was not needed to burn hydrogen at the pressures encountered in the test program, since the fuel burned directly from the fuel spray tubes. Some type of flame-promoting device might be used upstream of the fuel injectors to increase fuel-air mixing, but this increase in blockage might be used to better advantage by increasing the number of fuel injectors. Configuration A was not tested with a flameholder.

Effect of combustor length. - Combustion efficiencies are plotted in figure 7 for configuration A with a 16-inch combustor length (fuel spray tubes to water quench). The water quench spray was approximately at the end of the cone diffuser. The lower pressure range (13.2 to 24.0 in. Hg abs) was chosen to impose severe combustor condition. The measured combustion efficiencies for the 16-inch length (maximum of 96 percent) were slightly higher than or equal to those with the 28-inch combustor length. Configuration B was not tested with different combustor lengths.

In some ram-jet engine nomenclature, the combustion chamber is defined as the distance from the end of the diffuser to the entrance of the exhaust nozzle. In configuration A, the diffuser ends at the beginning of the convergent nozzle, thereby making it a zero-length combustor.

Temperature profiles. - The temperature profiles at the exhaust-nozzle throat, uncorrected for radiation and recovery errors, are shown in figure 8. Profiles were drawn at 2100° F and every 300° F lower. The temperature profiles are plotted for configurations A and B and for two inlet-air temperatures with configuration A. The equivalence ratios were approximately 0.31 and the combustor length (fuel spray to thermocouples) was 26 inches for A and 36 inches for B. Configuration B demonstrated a hotter core than configuration A. Increasing the inlet-air temperature from 230° (fig. 8(a)) to 640° F (fig. 8(c)) resulted in a more uniform outlet profile.

Configuration B was the first configuration tested, and configuration A, the result of applying certain design principles learned from configuration B, was designed to give better distribution of the fuel with the entering air and thereby a more uniform outlet temperature. The fuel was injected farther upstream in the annular area where the velocity profile was more uniform. The profile at the end of the diffuser or fuel-injection station for configuration B was irregular because of the sharp 25° diffuser angle coupled with the higher blockage at the center of the spoke-design fuel injectors. At the same time, configuration A increased the number of injection holes, which also improved the fuel distribution. Figures 8(a) and (b) show the improvement in the temperature profile at the engine exhaust nozzle as a result of these design changes.

To show the temperature spread in another way, a mean average temperature spread ΔT_m was calculated and is plotted against equivalence ratio in figure 9.

$$\Delta T_m = \frac{\sum_{N=1}^{N=N} |T_{av} - T_{T.C.}|}{N}$$

where

$T_{T.C.}$ individual thermocouple reading

T_{av} arithmetical average of N thermocouple readings

Configuration A consistently had less spread than configuration B, particularly at higher equivalence ratios.

Comparison Between Methods of Determining Efficiency

In figures 4 to 7, it is evident that reasonably good agreement existed among the efficiencies determined from the three methods of measurements. The maximum difference between the heat-balance and the thermocouple efficiencies was approximately 8 percent, and the maximum difference between the heat-balance and the total-pressure method was approximately 11 percent. Efficiencies determined from direct thermocouple and total-pressure measurements were generally higher than the heat-balance efficiencies, indicating that the combustion process was essentially completed by the time the gases reached the thermocouple and pressure-rake stations.

The heat balance is probably the most accurately determined combustion efficiency of all the methods. It is a measure of the chemical heat released, however, and not that heat necessarily available for propulsive energy.

Ignition Characteristics

Starting. - Ignition was successful with a spark at all conditions encountered with the available facilities. Heat addition was noted in the engine before a measureable fuel flow was reached. The following table contains the most severe (lowest pressure, highest velocity) inlet conditions at which the engine was started.

Config- uration	Pressure, in. Hg	Temperature, °F	Velocity, ft/sec	Minimum measurable equivalence ratio
A	22.0	230	354	0.020
A	13.1	640	410	.020
B	18.6	230	296	.020
C	7.1	230	130	.035
C	8.8	230	166	.035

General operation. - The engine started very smoothly with no increase in noise. Pressure and temperature instrumentation were needed to determine whether combustion was taking place. No roughness or instability was encountered at any equivalence ratio or at any pressure over the range of 9.2 to 50.0 inches of mercury absolute. Burning was sustained from the minimum measurable fuel flow to 1.3 equivalence ratio. The uncooled centerbody taper, extending beyond the fuel spray tubes in configuration A, showed no damage except heat discoloration after 90 minutes of operation.

3912

SUMMARY OF RESULTS

The following results were obtained from the combustion of gaseous hydrogen fuel in a 16-inch-diameter ram-jet engine for a range of inlet-air pressures of 9 to 50 inches of mercury absolute, velocities of 340 to 110 feet per second, and temperatures of 120° , 230° , and 640° F:

1. Hydrogen was burned with a maximum of 96 percent efficiency in a 16-inch combustor length with no flameholder, and at a combustor inlet pressure of 21 inches of mercury absolute.
2. Hydrogen demonstrated no combustion limits or instabilities when no flameholders were used over a pressure range of 9 to 50 inches of mercury absolute and equivalence ratios of 0.08 to 1.30.
3. The hydrogen combustor ignited at pressures as low as 7 inches of mercury absolute with spark ignition, no flameholder, inlet velocity of 130 feet per second, and air temperature of 230° F.

Lewis Flight Propulsion Laboratory
National Advisory Committee for Aeronautics
Cleveland, Ohio, October 26, 1955

APPENDIX - DATA REDUCTION METHODS

SYMBOLS

A	area, sq ft
c_F	area flow coefficient
g	acceleration of gravity, 32.2 ft/sec ²
ΔH	enthalpy rise of exhaust products, Btu/lb air
M	Mach number
N	number of thermocouples
p	static pressure, in. Hg abs
p_t	total pressure, in. Hg abs
R	gas constant, ft/ ^o R
ΔT_m	mean temperature deviation, ^o F
ΔT_R	radiation error, ^o F
T	static temperature, ^o R
$T_{T.C.}$	temperature measured by thermocouple, ^o R
T_t	total temperature, ^o R
w	weight flow
w_a	weight flow of air, vitiated or nonvitiated, lb/hr
w_f	weight flow of fuel, lb/hr
ϕ	equivalence ratio
γ	ratio of specific heats
η_b	combustion efficiency, percent

Subscripts:

n nozzle exit

t total

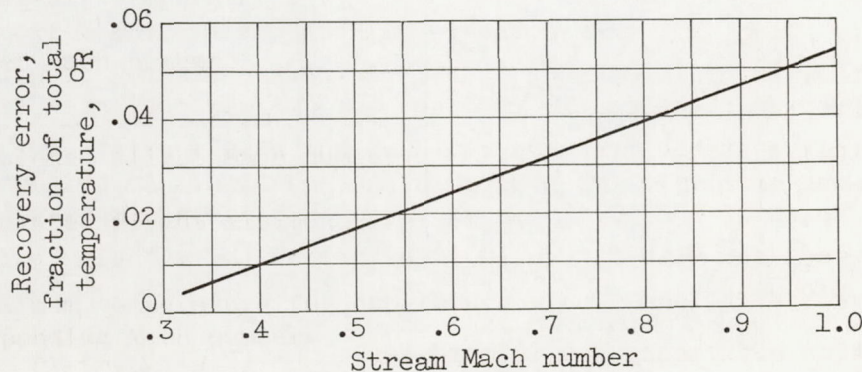
w weighted

Direct-thermocouple combustion efficiency. - The thermocouple readings were corrected for radiation and recovery errors as outlined in reference 5. The conduction loss was assumed negligible for an uncooled stem. The wire calibration was neglected because the thermocouples were burned out in each run. A wire emissivity of 0.8, a wire diameter of 0.020 inch, a nonluminous flame, and a low duct-wall temperature were used in the general radiation-error equation to obtain the working equation

$$\Delta T_R \approx 0.557 \left(\frac{T_{T.C.}}{1000} \right)^{3.82} \frac{1}{\sqrt{M_n P_n}}$$

The approximation sign is used because the analysis is for a wire cylinder instead of the short twisted thermocouple junction that was actually used. Radiation errors were about: 200° F for a reading of 2300° F, 120° F for a reading of 2000° F, and 20° F for a reading of 1000° F.

The recovery error is that fraction of the total temperature not recovered by a thermocouple wire and is a function of Mach number. A value for the recovery error was picked off the experimental curve shown here:



To mass-weight the thermocouples, the following assumptions were made:

1. Static pressure was constant across the plane of the thermocouples. Total pressure was measured with a 2 to 3 percent profile; therefore, Mach number and static pressure would also be constant, assuming a value of γ varying with the temperature profile.
2. Conditions at the nozzle throat were the same as those at the thermocouple plane 1/4 inch downstream.
3. Each thermocouple measured an area equal to A_n/N . This assumption was checked by measuring equal temperature areas of profiles as in figure 8, mass-weighting these areas, and calculating a combustion efficiency; the profile method agreed with the equal-area method.

A mass-weighted temperature was then defined as

$$T_{t,w} \equiv T_t \left(\frac{w}{w_n/N} \right)$$

where w is the actual weight flow through an area A_n/N , whose temperature is the corrected thermocouple temperature T_t . The average flow through A_n/N area was w_n/N . Substituting the continuity equation for the weight flows gave

$$T_{t,w} = T_t \sqrt{\frac{T_{t,n}}{T_t} \frac{\gamma R_n}{\gamma_n R} \frac{1 + \frac{\gamma - 1}{2} M^2}{1 + \frac{\gamma_n - 1}{2} M^2}}$$

The values of $T_{t,n}$, γ_n , and R_n were bulk values evaluated from heat-balance combustion efficiencies; γ and R were evaluated from the individual corrected thermocouple reading T_t . M was evaluated from a measured total-to-static pressure ratio at the nozzle exit. The accuracy of M was of little importance in the equation. An arithmetical average was taken of the $T_{t,w}$ values, and this average mass-weighted temperature was used with figure 10 to determine the enthalpy rise of the exhaust products.

Combustion efficiency was defined as

$$\eta_b \equiv \frac{\Delta H \times 100}{51,571 \frac{w_f}{w_a}}$$

Total-pressure combustion efficiency. - The continuity equation was written for the convergent-nozzle exit using total temperature, total pressure, and a flow area coefficient.

$$\sqrt{T_{t,n}} = \frac{c_F p_{t,n} A_n M_n \sqrt{\frac{\gamma_{ng}}{R_n}}}{w_n \left(1 + \frac{\gamma_n - 1}{2} M_n^2 \right)^{\frac{\gamma_n + 1}{2(\gamma_n - 1)}}}$$

If the ratio of the wall static pressure, measured 1 inch downstream of the nozzle, to the average total pressure measured by the rake was more than the critical pressure ratio, the nozzle was assumed choked. The value of γ varied from 1.40 to 1.25 depending on the temperature and gas composition at the nozzle exit. A value of 0.98 was chosen for c_F from reference 4 because the nozzle could not be calibrated with cold flow owing to the limited exhaust facilities. The measured nozzle area of 101.4 square inches was reduced by 2.8 square inches to correct for the blockage of the pressure rake. Substituting these values gave the following equation

$$\sqrt{T_{t,n}} = 9.67 \times 10^5 \frac{p_{t,n}}{w_n} \sqrt{\frac{\gamma_n}{R_n}} \left(\frac{\gamma_n + 1}{2} \right)^{\frac{\gamma_n + 1}{2(1-\gamma_n)}}$$

As the pressure rake was designed with probes in centers of equal areas, an arithmetical average of the rake was used for $p_{t,n}$. By assuming 100-percent combustion efficiency, ideal values of γ_n and R_n were dependent only upon equivalence ratio.

The value $T_{t,n}$ was then used with figure 10 to obtain the enthalpy rise of the exhaust products and, thus, the combustion efficiency.

REFERENCES

1. Olson, Walter T., and Gibbons, Louis C.: Status of Combustion Research on High-Energy Fuels for Ram Jets. NACA RM E51D23, 1951.
2. Silverstein, Abe, and Hall, Eldon W.: Liquid Hydrogen as a Jet Fuel for High-Altitude Aircraft. NACA RM E55C28a, 1955.

3. Cervenka, A. J., and Miller, R. C.: Effect of Inlet Air Parameters on Combustion Limit and Flame Length in 8-Inch-Diameter Ram-Jet Combustion Chamber. NACA RM E8C09, 1948.
4. Krull, H. George, and Steffen, Fred W.: Performance Characteristics of One Convergent and Three Convergent-Divergent Nozzles. NACA RM E52H12, 1952.
5. Scadron, Marvin D., Warshawsky, Isidore, and Gettleman, Clarence C.: Thermocouples for Jet-Engine Gas Temperature Measurement. Proc. Instr. Soc. Am., Paper No. 52-12-3, vol. 7, 1952, pp. 142-148.

TABLE I. - PERFORMANCE OF HYDROGEN IN A 16-INCH-DIAMETER RAM-JET ENGINE

Combustor length from fuel injectors		Hydrogen weight flow, lb/hr	Equivalence ratio	Combustor inlet air			Exhaust-nozzle pressure ratio	Combustion efficiency		
To quench spray nozzles	To pressure rake and thermocouples			Pressure, in. Hg abs	Temperature, °F	Velocity, ft/sec		Heat balance	Total pressure	Bare-wire thermocouples
Run 1: Configuration A, 0.5 nozzle, no flameholder										
34	26	239 288 250 411 462 497 555 633 862 1095 1322	0.150 .181 .219 .257 .289 .311 .346 .395 .539 .685 .827	22.7 23.6 25.2 26.8 28.0 29.2 31.8 33.1 36.8 42.2 45.0	232 232 233 233 233 234 234 234 234 237	246 237 223 209 200 192 177 170 153 134 125	1.51 1.55 1.57 1.61 1.60 1.63 1.76 1.81 1.87 2.06 2.16	51.1 51.9 59.9 71.3 73.2 77.9 85.2 89.2 92.6 95.4 95.1	53.5 58.0 67.3 77.5 74.7 79.0	
↓	↓								102.4	
Run 2: Configuration A, 0.5 nozzle, no flameholder										
28	26	236 288 350 394 450 546 640 754 947 1076 1336 1626	0.228 .260 .299 .324 .360 .416 .473 .543 .662 .740 .907 1.060	28.8 29.9 31.0 32.0 33.1 35.4 37.3 39.4 42.3 44.3 47.2 50.5	642 640 640 639 639 639 641 642 644 643 645 643	317 304 293 285 273 258 246 232 217 203 192 184	1.85 1.92 1.92 1.94 1.95 1.97 1.98 1.97 2.00 2.07 2.10 2.02	85.7 87.5 84.6 86.8 87.0 87.1 95.3 95.7 91.9 95.9 94.8 90.1	88.0 91.0 88.8 90.4 90.2	
↓	↓									
Run 3: Configuration B, 0.5 nozzle, no flameholder										
44	36	260 339 391 513 624 706 836 948 1101 1266 1576 1569	0.143 .185 .243 .280 .342 .387 .459 .521 .605 .700 .864 .860	26.4 27.7 29.8 32.8 34.9 36.7 39.0 41.0 43.1 45.7 48.4 48.2	119 120 121 120 120 120 121 122 123 124 122 122	202 194 180 164 154 146 138 131 125 117 111 112	1.61 1.67 1.81 1.96 2.05 2.12 2.22 2.18 2.28 2.42 1.97 1.78	88.7 81.5 88.7 91.8 88.6 94.5 93.2 93.7 92.1 92.0 87.9 87.7	88.5 82.1 88.5 89.4 94.0 94.0 90.2 99.5	
↓	↓									

TABLE I. - Continued. PERFORMANCE OF HYDROGEN IN A 16-INCH-DIAMETER RAM-JET ENGINE

Combustor length from fuel injectors		Hydrogen weight flow, lb/hr	Equivalence ratio	Combustor inlet air			Exhaust-nozzle pressure ratio	Combustion efficiency		
To quench spray nozzles	To pressure rake and thermocouples			Pressure, in. Hg abs	Temperature, °F	Velocity, ft/sec		Heat balance	Total pressure	Bare-wire thermocouples
Run 4: Configuration B, 0.5 nozzle, no flameholder										
44	36	243	0.153	25.0	232	223	1.52	87.8		92.4
		311	.193	26.3	237	216	1.60	79.3		85.7
		331	.205	27.1	233	209	1.64	84.2		93.7
		278	.297	30.4	232	186	1.82	90.1		91.5
		542	.340	32.0	234	175	1.89	91.6		90.4
		622	.390	31.9	234	176	1.90	88.4		
		678	.425	33.7	234	166	1.89	85.8		
		851	.533	37.0	234	152	2.12	90.8		
		1033	.647	39.7	235	142	2.19	91.4	93.2	
		1194	.748	42.0	236	134		89.4		
		1255	.789	42.7	238	132		88.3		
		1547	.971	45.7	236	123		87.0		
Run 5: Configuration B, 0.5 nozzle, no flameholder										
44	36	167	0.107	23.7	247	238	1.64			57.0
		234	.146	24.6	234	229	1.63			72.0
		260	.164	25.4	228	219	1.65			91.0
		319	.199	26.8	223	207	1.71			78.0
		412	.260	29.1	231	191	1.85			83.0
		464	.293	30.0	238	186	1.91			83.5
		498	.317	30.7	235	180	2.16			85.5
Run 6: Configuration B, 0.5 nozzle, no flameholder										
44	36	255	0.243	28.1	650	320	1.84	99.4		80.3
		328	.289	29.3	651	307	1.93	90.5		76.0
		357	.306	29.8	652	303	1.99	90.8		79.0
		439	.358	31.5	651	286	2.04	88.1		
		509	.402	32.8	651	275	2.10	90.9		
		575	.443	34.1	651	264	2.14	91.1		
		734	.542	37.0	651	243	1.96	94.1		
		817	.594	38.1	653	237	2.02	93.6		
		895	.642	39.1	654	231	2.07	94.0		
		999	.708	40.4	654	224	2.13	92.4		
		1128	.789	41.5	654	217	2.20	90.2	91.7	
		1320	.909	42.9	651	210	2.28	86.0	96.8	

3912

TABLE I. - Continued. PERFORMANCE OF HYDROGEN IN A 16-INCH-DIAMETER RAM-JET ENGINE

Combustor length from fuel injectors	Hydrogen weight flow, lb/hr	Equivalence ratio	Combustor inlet air			Exhaust-nozzle pressure ratio	Combustion efficiency		
			Pressure, in. Hg abs	Temperature, °F	Velocity, ft/sec		Heat balance	Total pressure	Bare-wire thermocouples
Run 7: Configuration A, 1.0 nozzle, no flameholder									
28	26	79	0.198	13.2	628	336	None	88.4	88.4
		114	.242	13.9	618	315		82.7	84.5
		140	.275	14.1	618	311		80.8	81.8
		181	.325	14.4	618	305		71.9	69.8
		213	.365	14.9	616	294		71.8	73.8
		246	.406	15.4	615	284		74.1	73.5
		299	.472	15.9	615	275		77.6	79.1
		335	.517	16.7	617	263		82.4	
		449	.659	18.8	619	234		91.5	
		544	.777	20.1	618	218		94.1	
		707	.980	22.0	621	200		90.1	
		794	1.088	22.6	623	195		85.4	
Run 8: Configuration B, 1.0 nozzle, no flameholder									
44	36	241	0.150	19.9	230	283	None	72.9	84.5
		307	.191	21.1	234	267		72.6	84.9
		340	.213	21.6	235	260		74.2	86.6
		444	.275	23.5	233	241		81.6	88.2
		460	.292	24.0	230	229		84.5	
		583	.349	26.9	230	217		87.5	
		674	.413	27.9	230	205		91.0	
		748	.461	28.8	238	199		91.5	
		797	.494	29.2	237	195		91.7	
		1037	.641	32.3	236	177		93.0	
		1199	.745	33.6	239	170		89.4	
		1325	.803	34.6	239	169		87.2	
Run 9: Configuration C, 1.0 nozzle, no flameholder									
	26	6.2	0.082	9.2	252	172	None		17.1
		9.1	.120	9.2	251	172			26.6
		11.6	.154	9.3	250	170			39.6
		14.1	.183	9.7	247	162			47.5
		18.4	.224	10.5	228	155			54.4
		21.6	.263	10.5	224	154			63.5
		23.9	.286	10.9	223	149			61.9
		27.4	.322	11.2	222	144			69.0
		30.4	.355	11.3	221	143			69.0
		34.0	.411	11.4	222	142			72.0

TABLE I. - Concluded. PERFORMANCE OF HYDROGEN IN A 16-INCH-DIAMETER RAM-JET ENGINE

Combustor length from fuel injectors	Hydrogen weight flow, lb/hr	Equivalence ratio	Combustor inlet air			Exhaust-nozzle pressure ratio	Combustion efficiency		
			Pressure, in. Hg abs	Temperature, °F	Velocity, ft/sec		Heat balance	Total pressure	Bare-wire thermocouples
Run 10: Configuration B, 0.5 nozzle, flameholder									
44	36								
		224	0.141	24.3	232	230	1.57	79.3	76.1
		315	.198	25.4	236	221	1.65	71.9	68.9
		372	.233	27.1	236	207	1.76	76.7	76.7
		453	.284	29.0	235	194	1.98	82.7	77.7
		520	.327	30.8	239	183	2.09	87.6	
		626	.394	33.0	241	171	2.24	86.6	95.6
		718	.449	35.3	235	160	2.36	94.5	98.4
		800	.500	36.6	231	153	2.44	92.2	97.9
		894	.559	38.3	232	147	2.48	92.0	97.7
		1069	.670	40.6	235	138	2.59	92.0	96.0
		1151	.721	40.5	235	139	2.24	96.9	95.8
		1457	.913	36.2	238	156	2.44	89.8	93.4
Run 11: Configuration A, no 1.0 nozzle, no flameholder									
16	14								
		102	0.209	13.6	616	319	None	73.8	
		128	.243	13.8	618	313		71.1	
		169	.293	14.5	615	300		75.8	
		206	.338	16.2	615	269		83.7	
		251	.394	18.7	618	234		82.1	
		292	.444	17.6	618	249		85.7	
		305	.464	17.7	618	246		88.9	
		424	.609	19.6	616	223		88.3	
		498	.704	20.9	618	209		95.9	
		544	.762	21.4	618	204		95.8	
		619	.855	22.3	618	196		91.6	
		862	1.161	24.0	622	182		81.4	

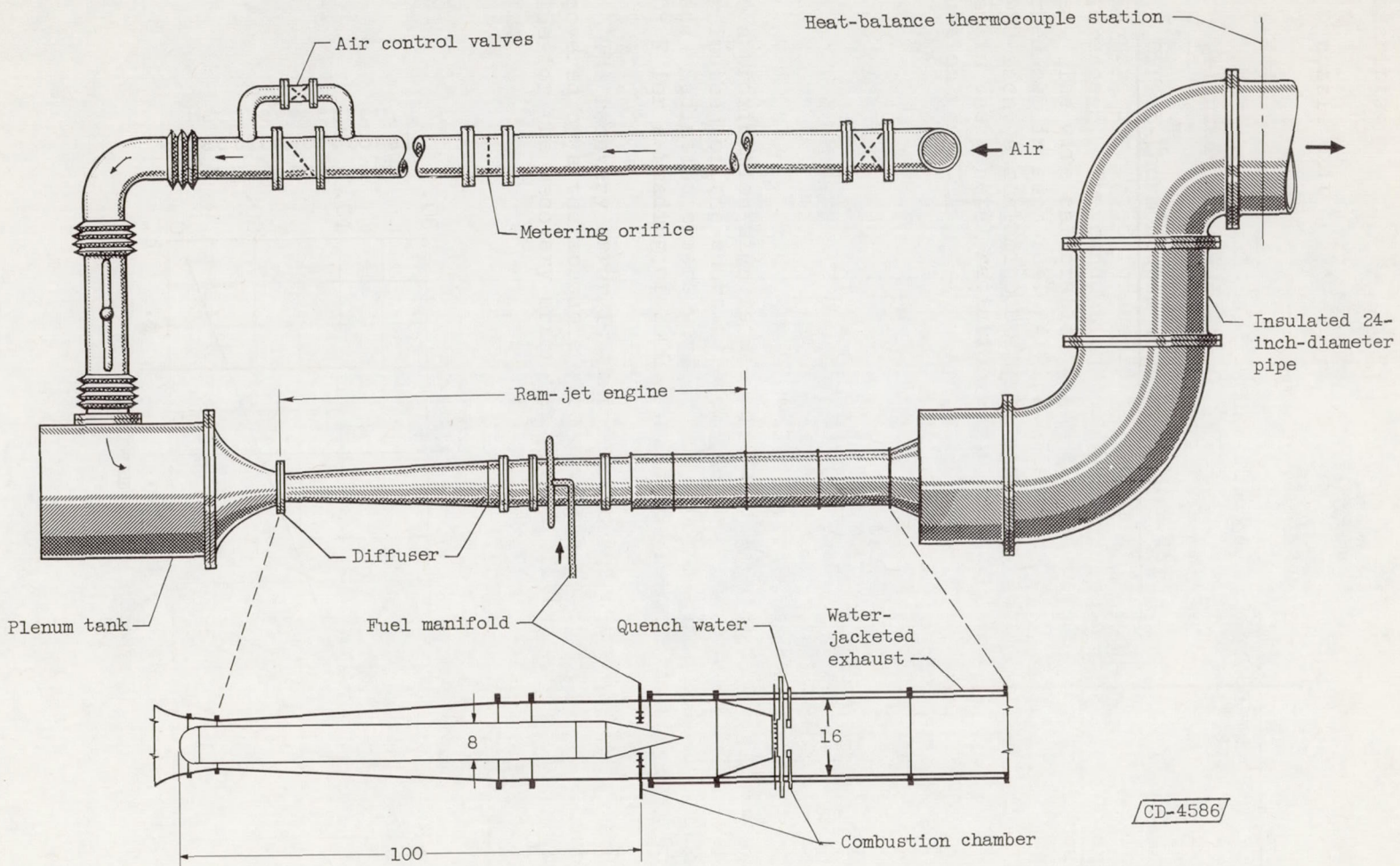


Figure 1. - Installation of 16-inch-diameter ram-jet engine in connected-pipe facility.
(All dimensions in inches.)

CONFIDENTIAL

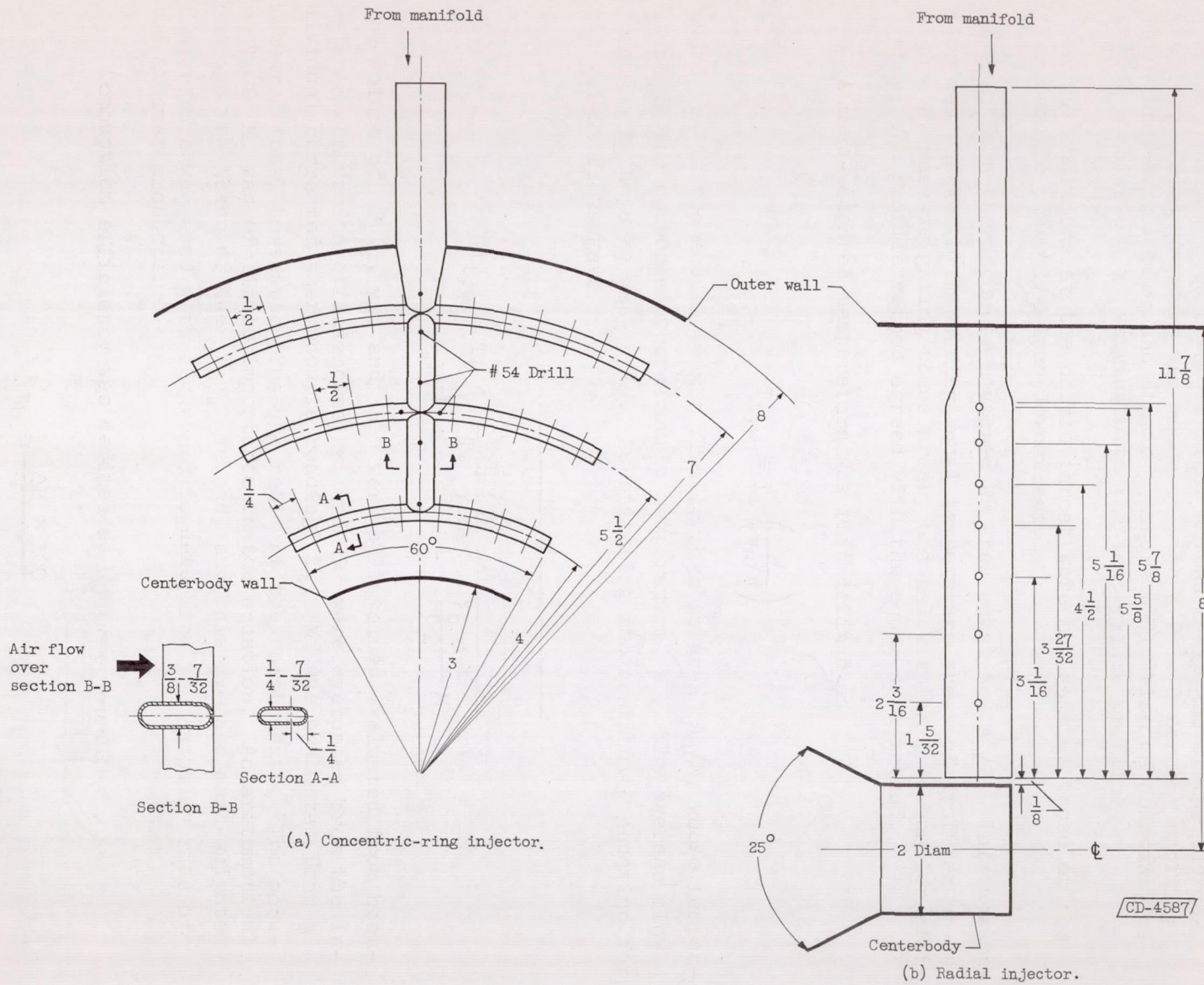
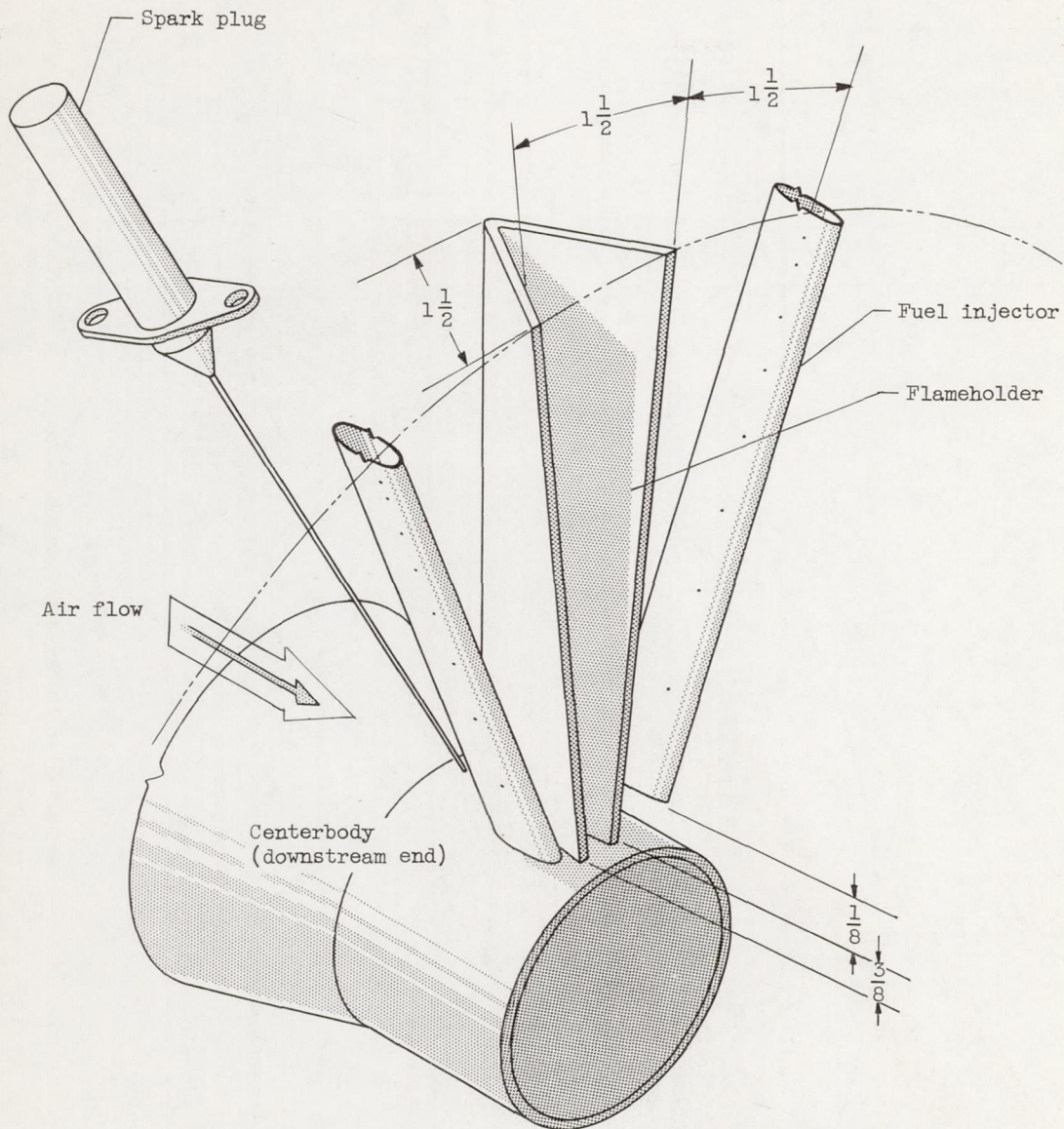


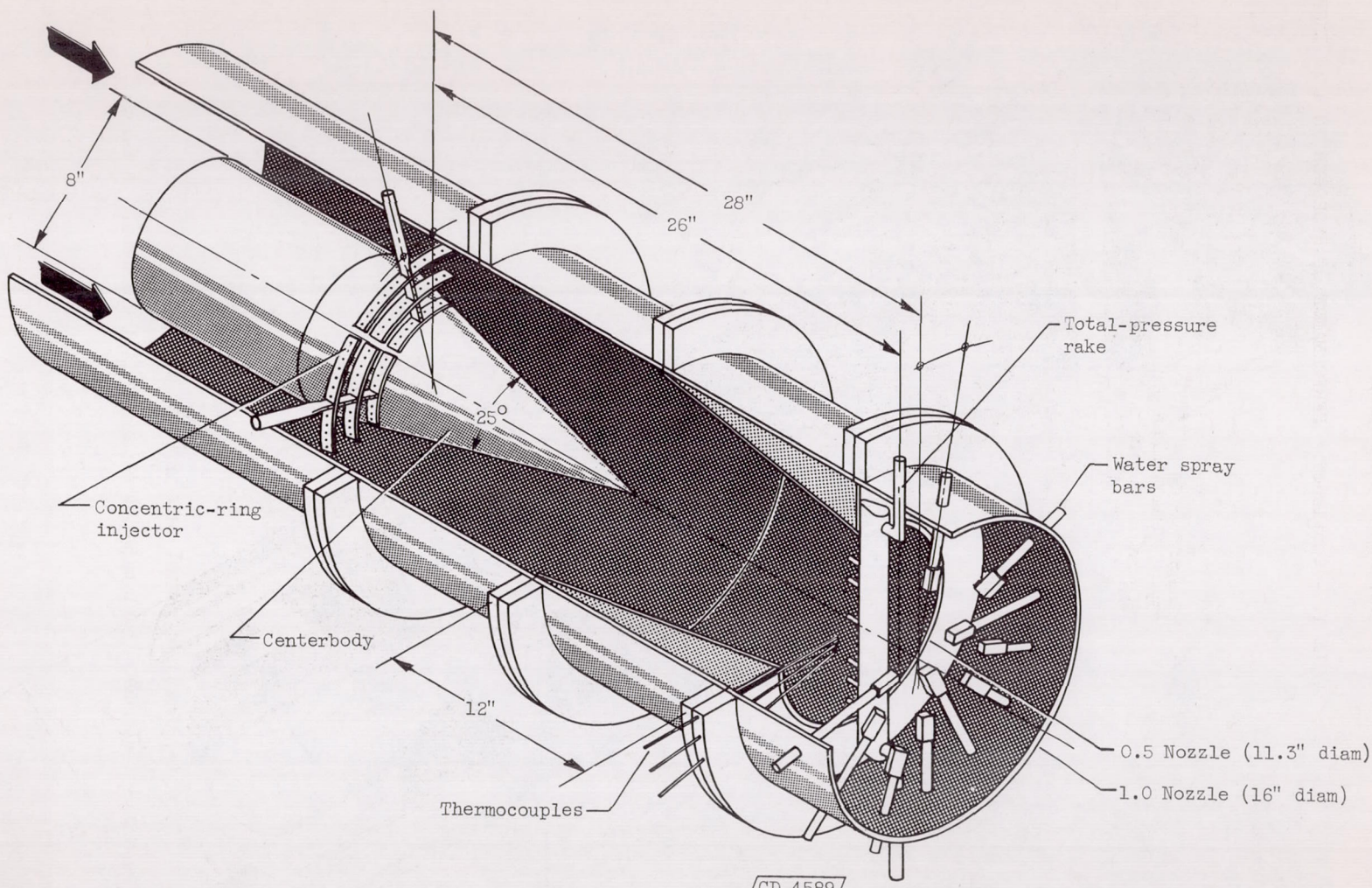
Figure 2. - Fuel-injector designs. (All dimensions in inches.)



(c) Detail of radial fuel injector and flameholder.

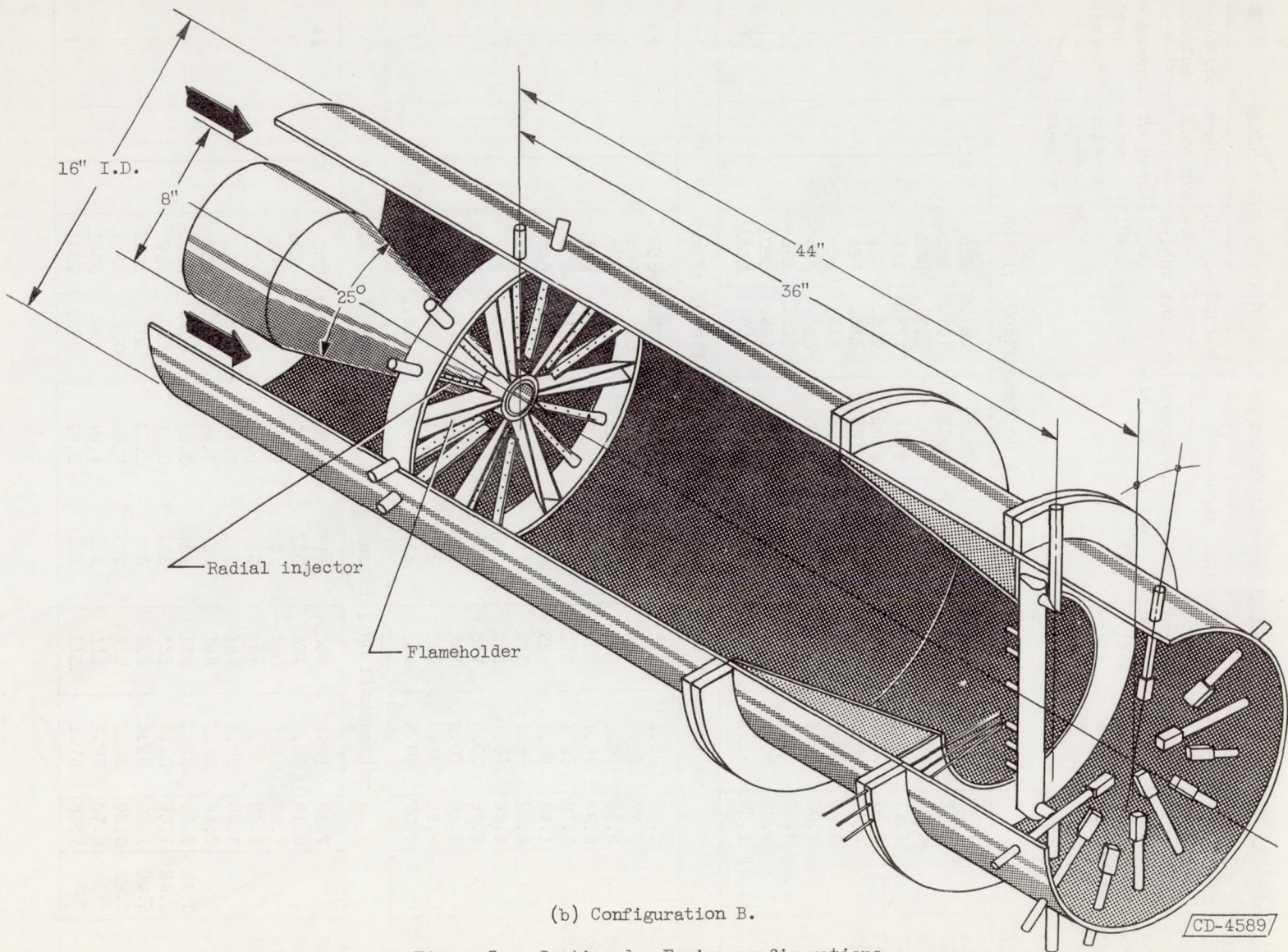
Figure 2. - Concluded. Fuel-injector designs. (All dimensions in inches.)

CONFIDENTIAL



(a) Configuration A.

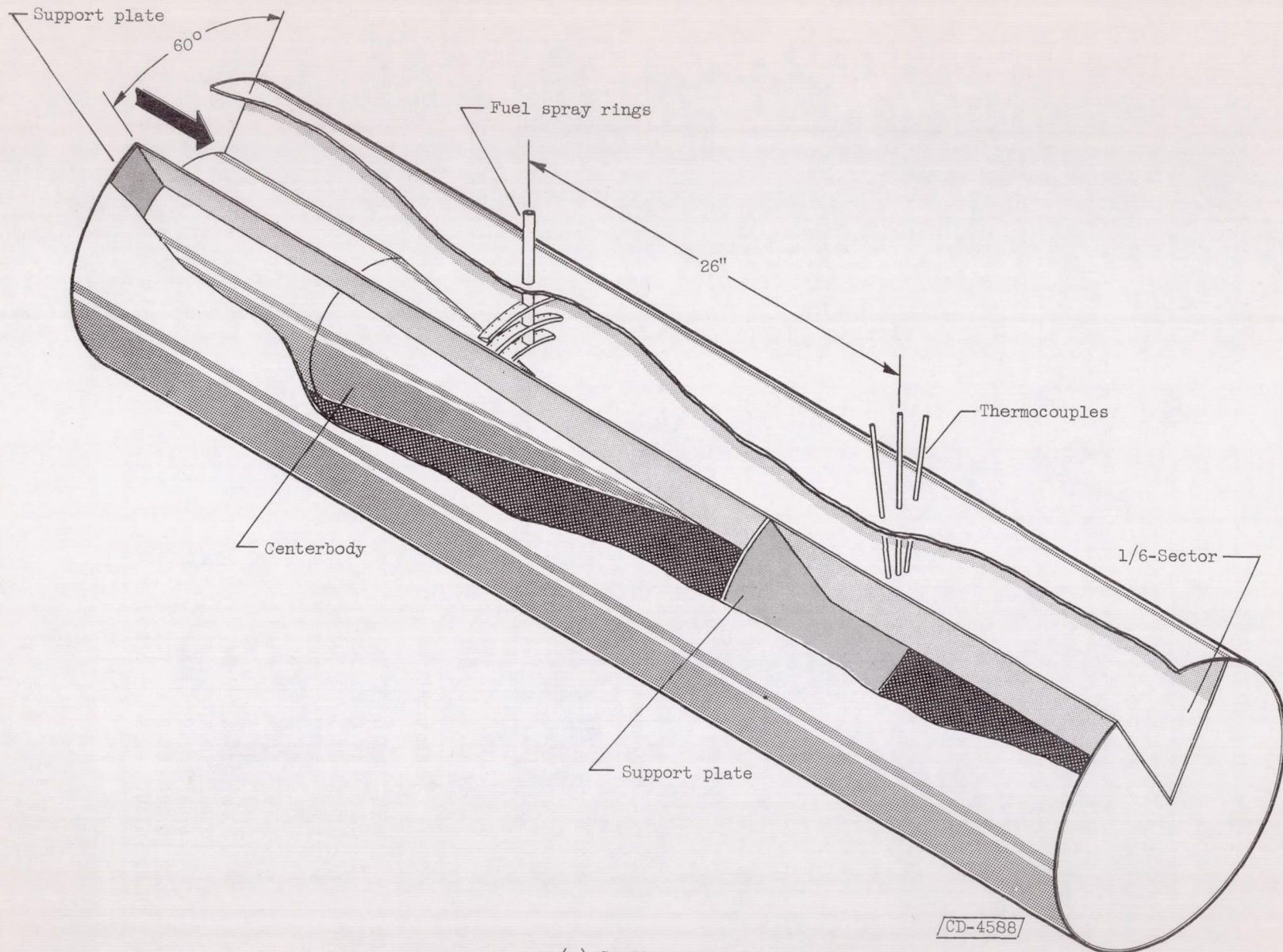
Figure 3. - Engine configurations.



(b) Configuration B.

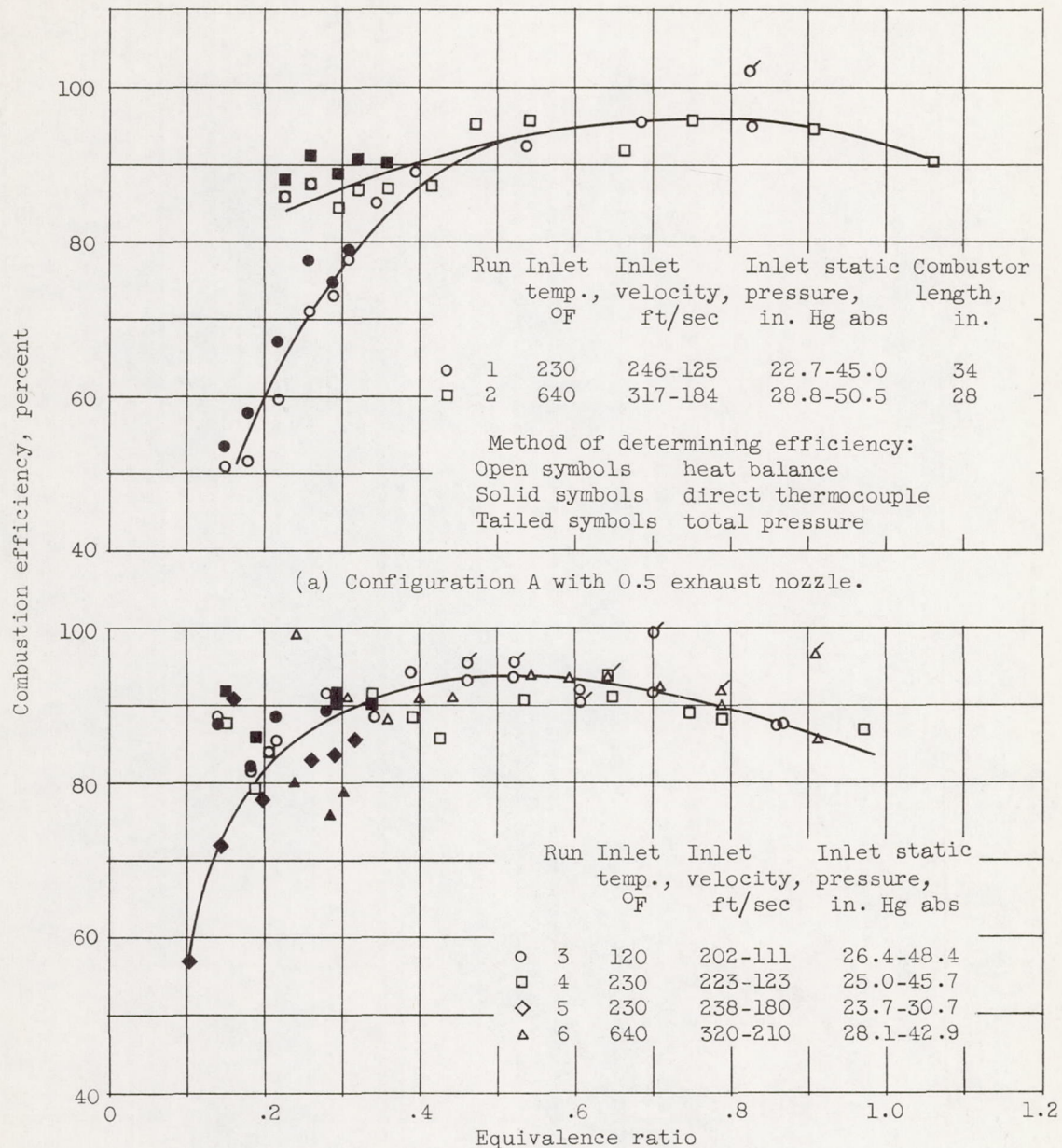
Figure 3. - Continued. Engine configurations.

CONFIDENTIAL



(c) Configuration C.

Figure 3. - Concluded. Engine configurations.



(b) Configuration B with 0.5 exhaust nozzle; combustor length, 44 inches.

Figure 4. - Effect of inlet-air temperature on combustor performance.

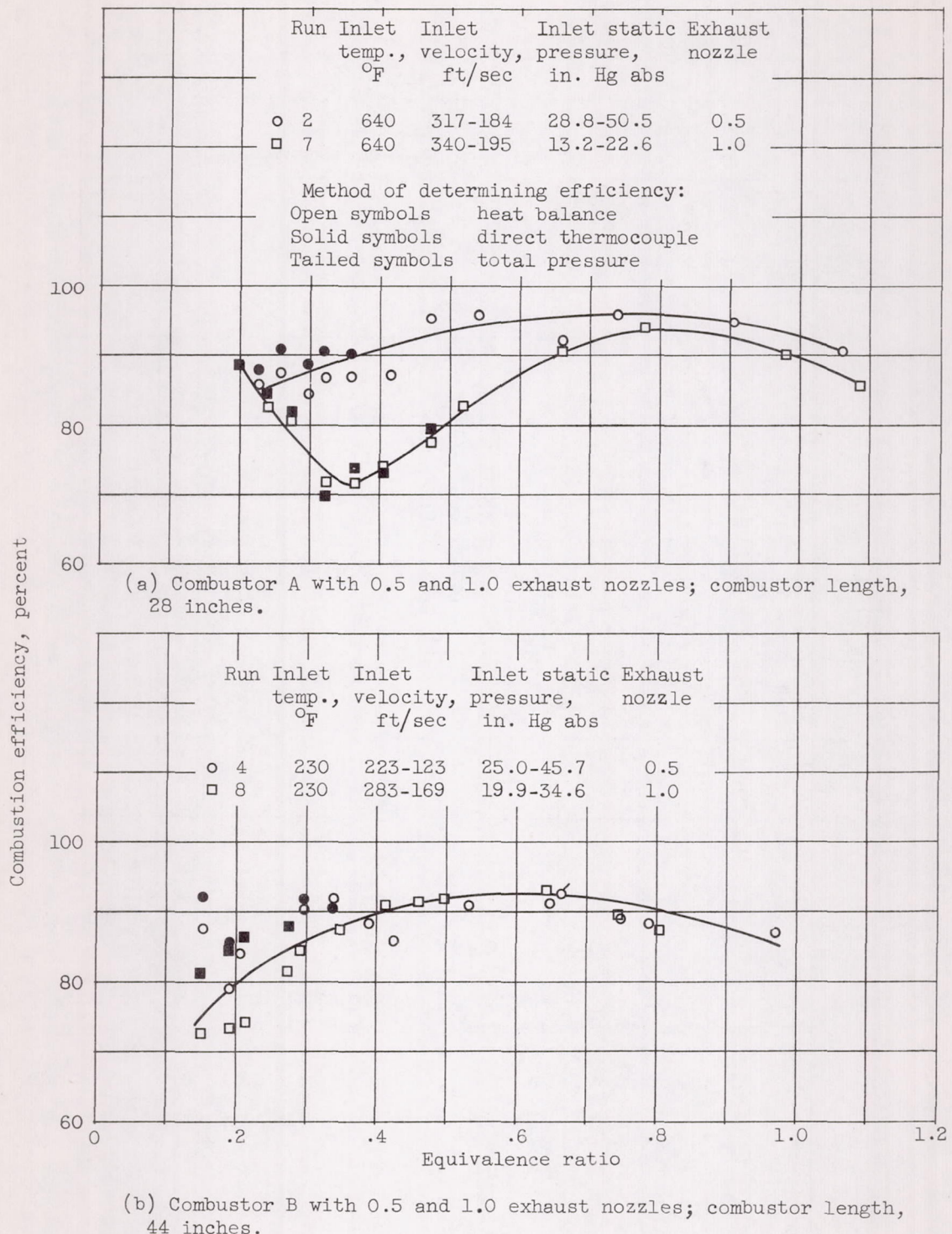
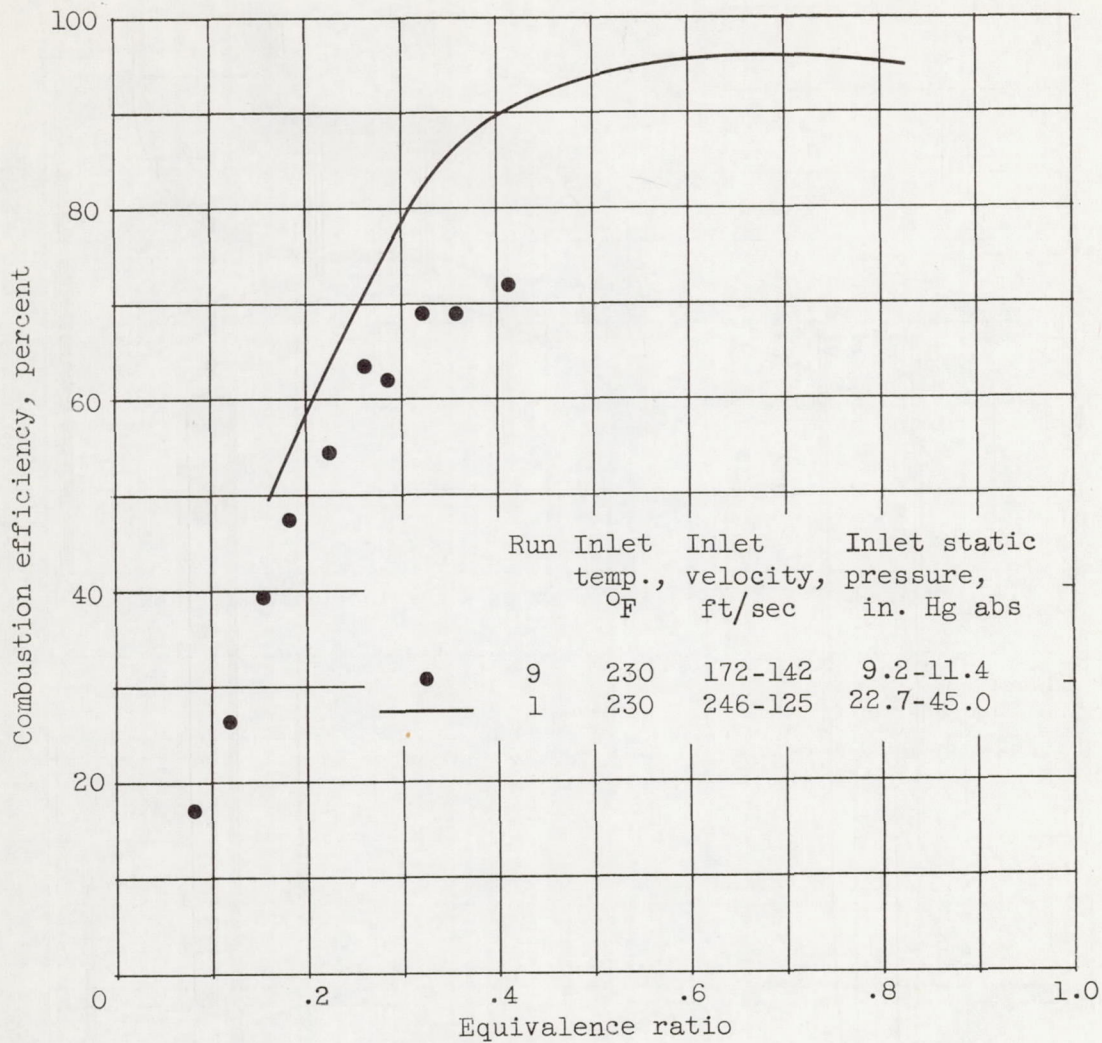


Figure 5. - Effect of pressure on combustor performance.



(c) Configuration C (1/6-sector of configuration A); efficiency determined from direct thermocouple measurements.

Figure 5. - Concluded. Effect of pressure on combustor performance.

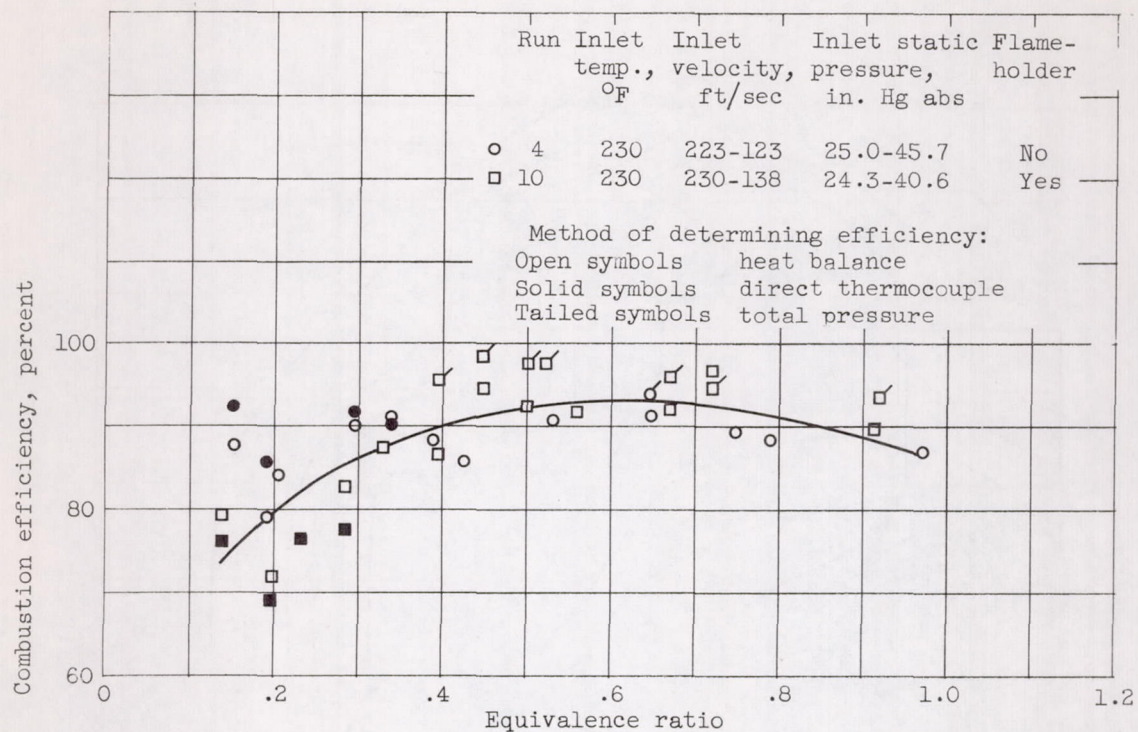


Figure 6. - Effect of flameholder on performance of configuration B with 0.5 exhaust nozzle.

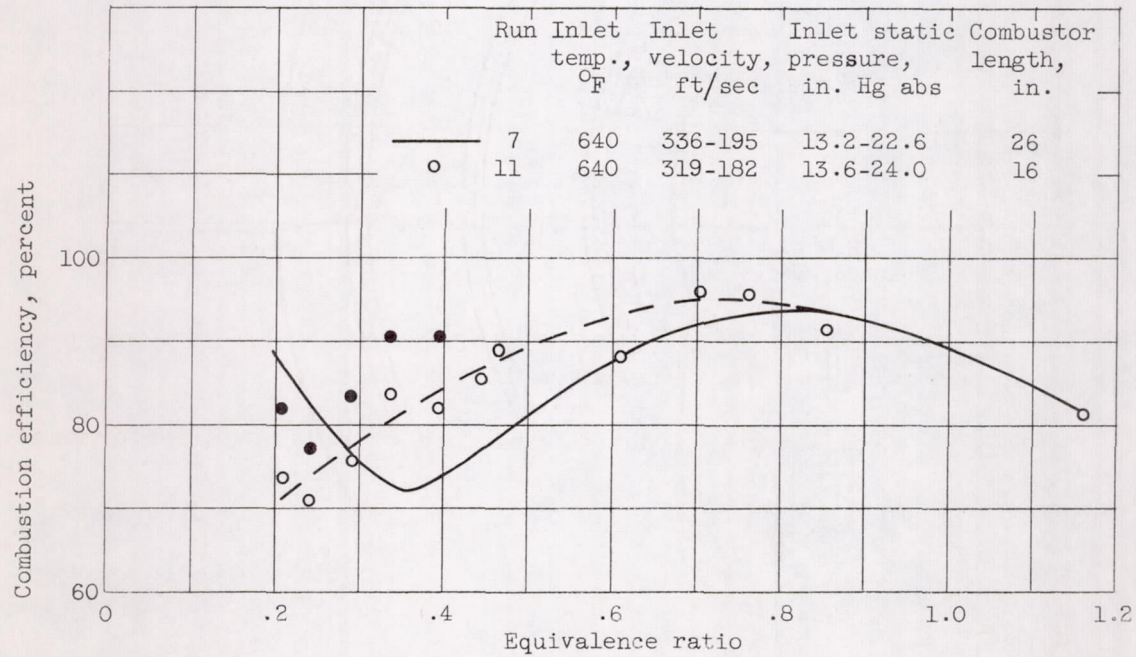
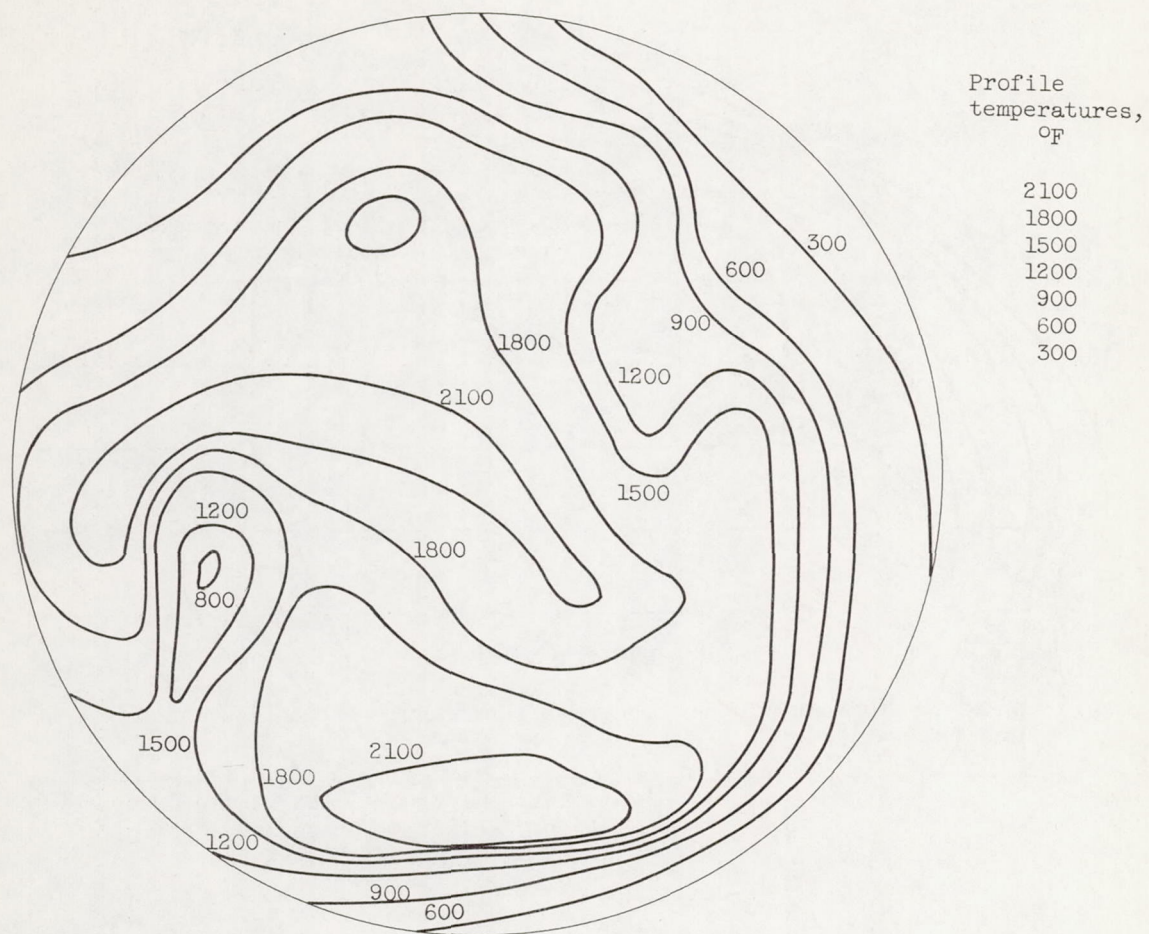
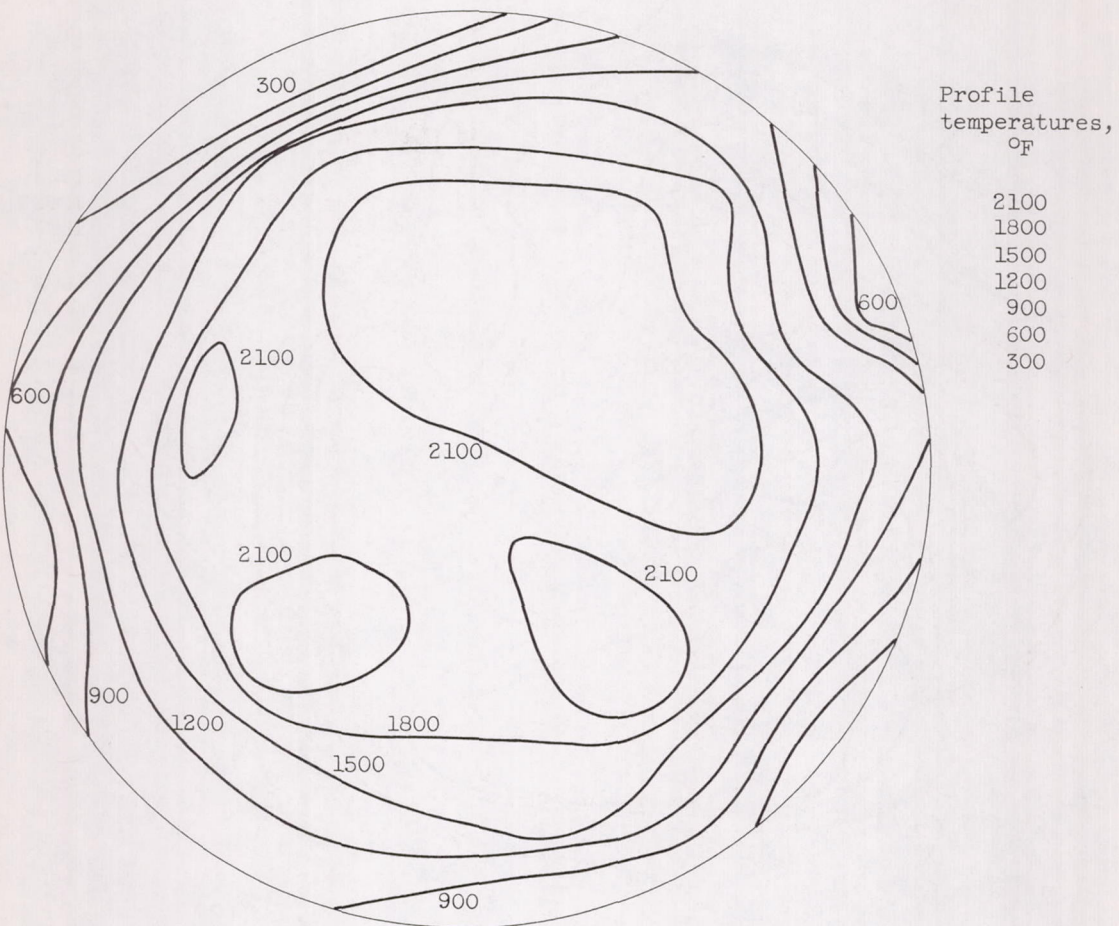


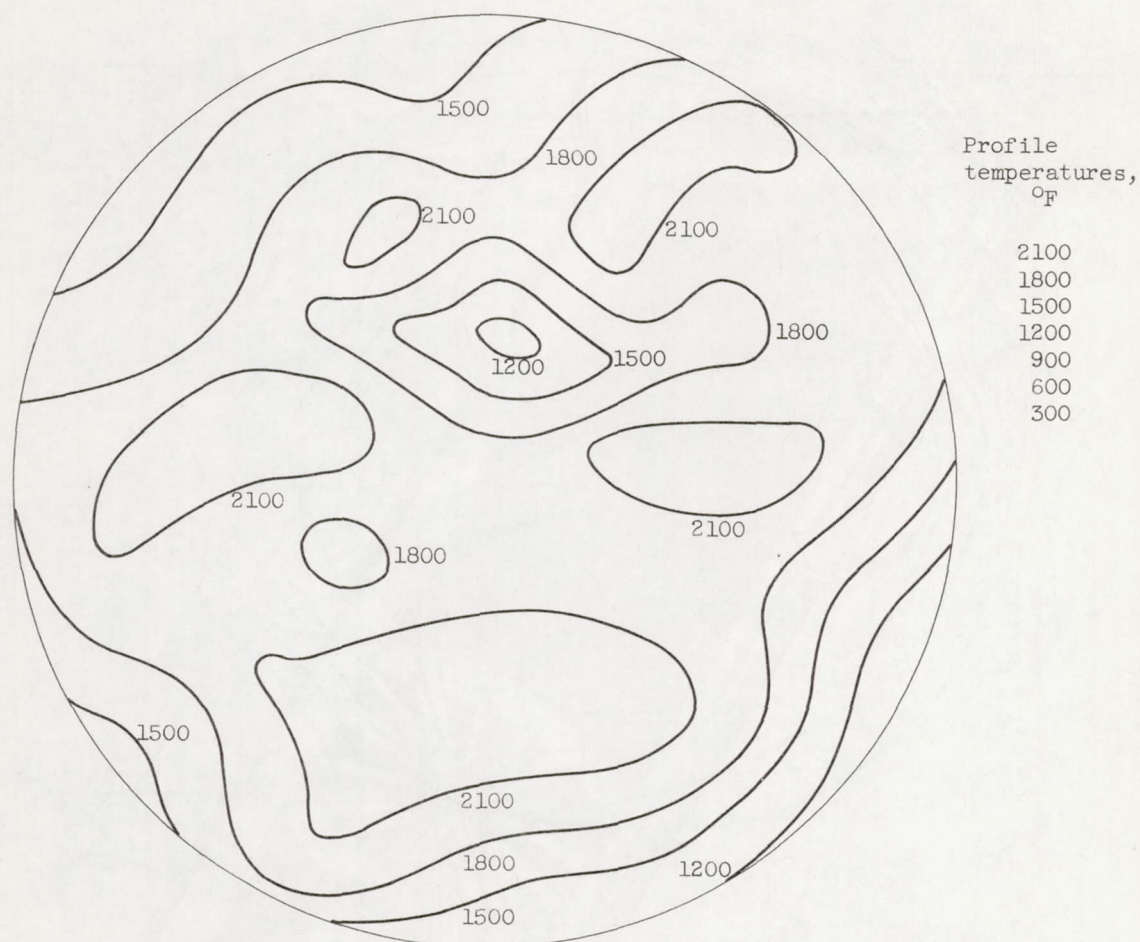
Figure 7. - Effect of combustor length on performance of configuration A.



(a) Configuration A; run 1. Exhaust nozzle, 0.5; combustor inlet air temperature, 230° F; combustor static pressure, 29.2 inches mercury absolute; equivalence ratio, 0.31.

Figure 8. - Temperature profiles at exhaust nozzle.





(c) Configuration A; run 2. Exhaust nozzle, 0.5; combustor inlet air temperature, 640° F; combustor static pressure, 33.1 inches mercury absolute; equivalence ratio, 0.276 + 0.083 vitiation correction.

Figure 8. - Concluded. Temperature profiles at exhaust nozzle.

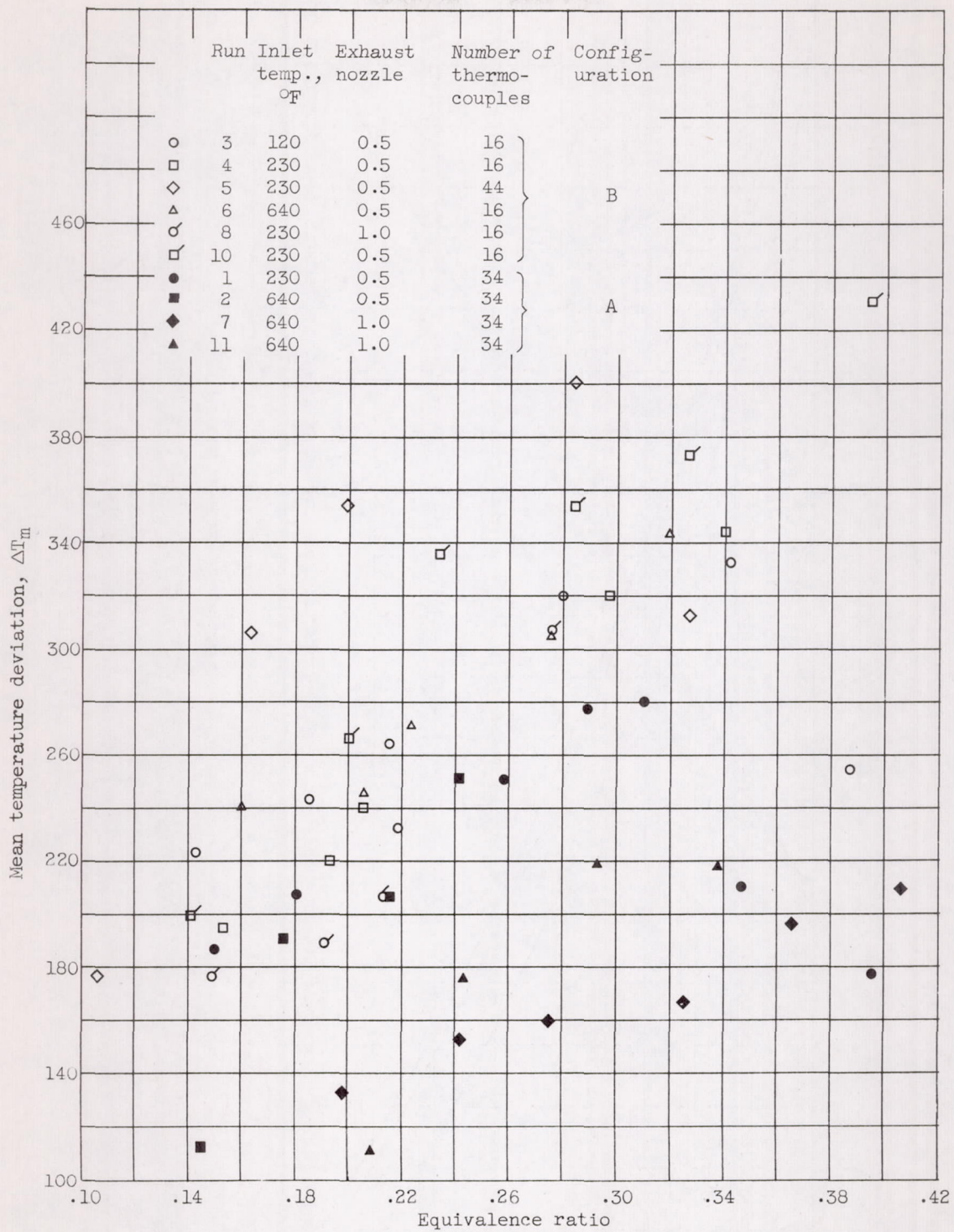


Figure 9. - Mean temperature deviation as a function of equivalence ratio.

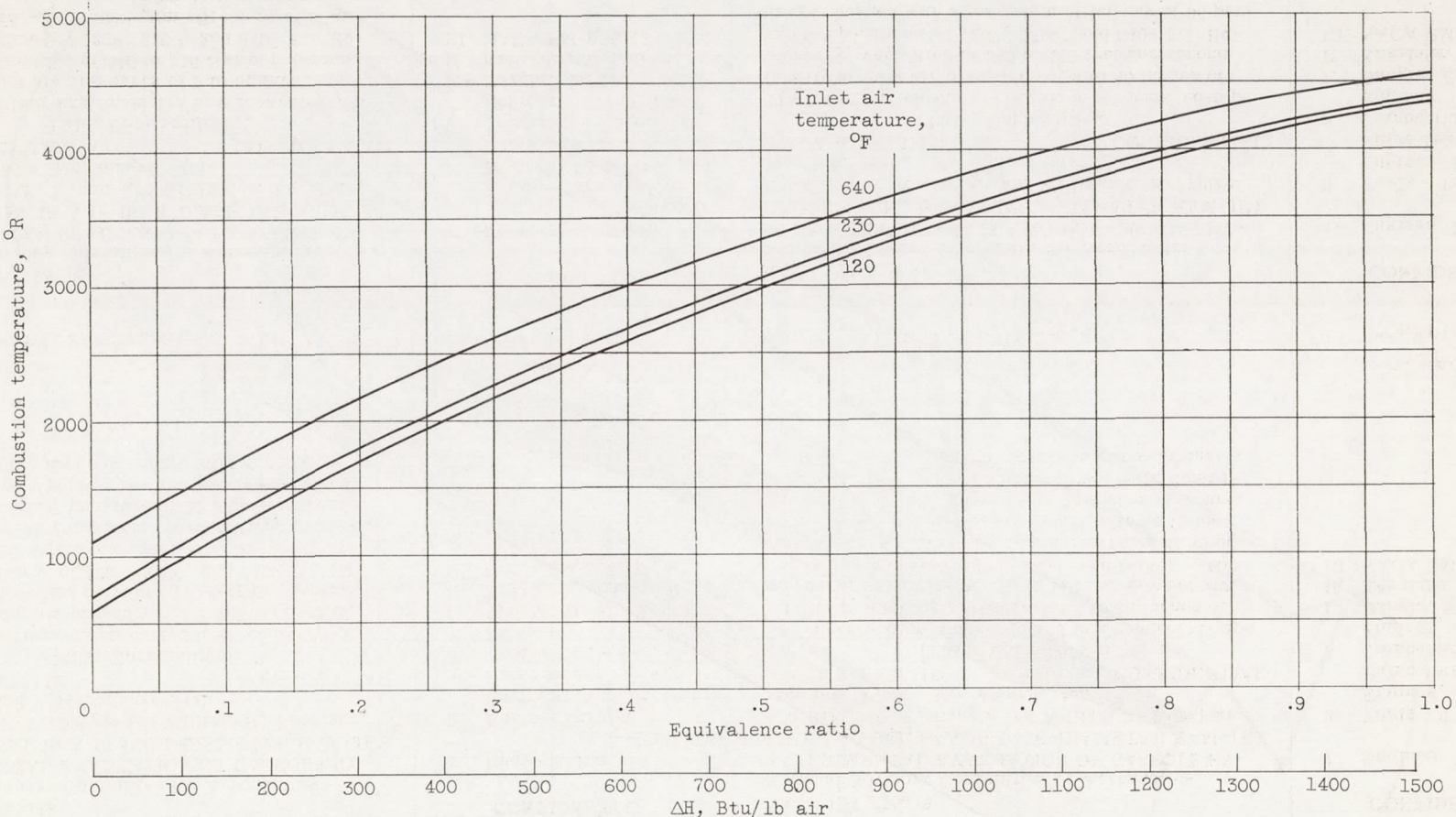


Figure 10. - Theoretical combustion temperature of gaseous hydrogen at 45° F and air temperatures of 120°, 230°, and 640° F. Combustion pressure, 2 atmospheres.

CONFIDENTIAL

NACA - Langley Field, Va.

CONFIDENTIAL

CONFIDENTIAL